New Phytologist

Research

Hydrogen isotope fractionation in carbohydrates of leaves and xylem tissues follows distinct phylogenetic patterns: a common garden experiment with 73 tree and shrub species

Philipp Schuler[1,2], Valentina Vitali[1], Matthias Saurer[1], Arthur Gessler[1,2], Nina Buchmann[2] and Marco M. Lehmann[1]

[1]Forest Dynamics, Swiss Federal Institute for Forest, Snow and Landscape Research WSL, Birmensdorf 8903, Switzerland; [2]Department of Environmental Systems Science, ETH Zurich, Zurich 8092, Switzerland

Author for correspondence:
Philipp Schuler
Email: philipp.schuler@wsl.ch

Received: *28 December 2022*
Accepted: *13 April 2023*

New Phytologist (2023) **239:** 547–561
doi: 10.1111/nph.18976

Key words: cellulose, hydrogen isotopes, photosynthesis, phylogeny, plant physiology, sugar, tree rings.

Summary

- Recent methodological advancements in determining the nonexchangeable hydrogen isotopic composition (δ^2H_{ne}) of plant carbohydrates make it possible to disentangle the drivers of hydrogen isotope (^2H) fractionation processes in plants.
- Here, we investigated the influence of phylogeny on the δ^2H_{ne} of twig xylem cellulose and xylem water, as well as leaf sugars and leaf water, across 73 Northern Hemisphere tree and shrub species growing in a common garden.
- ^2H fractionation in plant carbohydrates followed distinct phylogenetic patterns, with phylogeny reflected more in the δ^2H_{ne} of leaf sugars than in that of twig xylem cellulose. Phylogeny had no detectable influence on the δ^2H_{ne} of twig or leaf water, showing that biochemistry, not isotopic differences in plant water, caused the observed phylogenetic pattern in carbohydrates. Angiosperms were more ^2H-enriched than gymnosperms, but substantial δ^2H_{ne} variations also occurred at the order, family, and species levels within both clades. Differences in the strength of the phylogenetic signals in δ^2H_{ne} of leaf sugars and twig xylem cellulose suggest that the original phylogenetic signal of autotrophic processes was altered by subsequent species-specific metabolism.
- Our results will help improve ^2H fractionation models for plant carbohydrates and have important consequences for dendrochronological and ecophysiological studies.

Introduction

Isotope ratios of the nonexchangeable hydrogen in plant carbohydrates (δ^2H_{ne}; i.e. the hydrogen that is bound to carbon) are becoming an increasingly important proxy for the study of metabolic pathways (Cormier *et al.*, 2018; Sanchez-Bragado *et al.*, 2019; Schuler *et al.*, 2022; Wieloch *et al.*, 2022), the origin of plant water (Kagawa, 2022), plant internal carbohydrate dynamics (Lehmann *et al.*, 2021), and past climatic conditions (Yapp & Epstein, 1982; Augusti *et al.*, 2008). However, the actual ^2H fractionation processes influencing the δ^2H_{ne} of sugars and cellulose in autotropic and heterotrophic tissues remain elusive (Badea *et al.*, 2021; Schönbeck & Santiago, 2022). Recent studies have highlighted that the transfer of the ^2H signal from leaf sugars to leaf cellulose (Holloway-Phillips *et al.*, 2022) or from source water to tree-ring cellulose (Arosio *et al.*, 2020b; Lehmann *et al.*, 2022; Vitali *et al.*, 2022) varies both within and among species and is also dynamic over time. However, systematic studies on potential phylogenetic effects on δ^2H_{ne} in trees are still missing.

The isotopic composition of source water, which is mostly taken up by plant roots (Ziegler, 1989), depends on the isotopic composition of the rain, which is strongly influenced by air temperature and the distance to the ocean, among other factors (Craig, 1961; Dansgaard, 1964). Although a ^2H fractionation effect was recently observed during root water uptake in *Fagus sylvatica* L. (Barbeta *et al.*, 2020), the observed fractionation process might have been a methodological artefact potentially caused by the small amount of extracted water (Diao *et al.*, 2022). Generally, however, source water uptake by roots is thought to have no distinct ^2H fractionation effect (White, 1989). Subsequently, water is transported into leaves, where ^2H becomes enriched in the leaf water due to evaporative enrichment (Farquhar *et al.*, 2007) and the ^2H signal is mixed with the isotopic signal of atmospheric water vapour and rain (Lehmann *et al.*, 2018; Cernusak *et al.*, 2022; Kagawa, 2022). The ^2H fractionation processes in plant water are mainly the result of physical processes and can be modelled accurately (Cernusak *et al.*, 2016). Such models consider the transfer of δ^2H of source and leaf water to the δ^2H_{ne} of tree-ring cellulose (Roden *et al.*, 2000; Roden & Ehleringer, 2000). By contrast, the metabolic ^2H fractionation processes that shape δ^2H in plant carbohydrates are poorly understood. Large variation can occur in the δ^2H of different

plant organic compounds, caused by different ^2H fractionation processes during their biosynthesis (Luo & Sternberg, 1991; Zhou *et al.*, 2016; Baan *et al.*, 2023). One of the proposed main drivers of a ^2H fractionation in C_3 plants is proton production during the water-splitting process in the light-dependent reactions, which discriminates against the heavier ^2H isotope. This leads to a strongly depleted pool of reducing equivalences, such as NADPH (Luo *et al.*, 1991). Spatial and temporal variation in CO_2 uptake and assimilation in C_4 and CAM plants lead to significant metabolic changes and to a ^2H-enrichment in carbohydrates compared with in C_3 plants (Luo & Sternberg, 1991; Schuler *et al.*, 2022). Some of these processes may help to explain species-specific δ^2H variations in the carbohydrates of C_3 plants.

Furthermore, various heterotrophic ^2H fractionation processes occur during plant metabolism (Augusti *et al.*, 2008), altering the initial δ^2H_{ne} of the fresh assimilates (e.g. nonstructural carbohydrates (NSCs) in the form of sugar and starch) in the pathway to tree-ring cellulose formation (Kagawa & Battipaglia, 2022; Lehmann *et al.*, 2022). At the leaf level, heterotrophic ^2H fractionation processes within a species seem to be relatively constant under stable climatic conditions, and the δ^2H_{ne} of leaf sucrose can explain more than the half of the δ^2H_{ne} variation in leaf cellulose (Holloway-Phillips *et al.*, 2022). It is currently assumed that, similar to the isotopic exchange of oxygen isotopes between carbohydrates and xylem water during tree-ring formation (Epstein *et al.*, 1977; Cernusak *et al.*, 2005; Gessler *et al.*, 2009), the hydrogen of plants carbohydrates undergoes an isotopic exchange with the xylem water during cellulose formation (Augusti *et al.*, 2006, 2008). Furthermore, recent findings suggest that fundamental plant traits, such as seasonal leaf shedding behavior, significantly impact the δ^2H_{ne} of tree-ring cellulose (Arosio *et al.*, 2020b). Such effects may be caused by differences in ^2H fractionation processes (Lehmann *et al.*, 2022), but the mechanistic basis of these processes is not yet known. Several biochemical pathways probably influence the apparent autotrophic and heterotrophic ^2H fractionation, and they can be summarized as ε_{HA} (autotrophic ^2H fractionation, between leaf water and sugar) and ε_{HE} (heterotrophic ^2H fractionation, between sugars and cellulose). Due to the complexity of these interactions, it is not well-understood which processes drive ε_{HA} and ε_{HE}, and how this differs among plant species or functional groups.

Phylogenetic (evolutionary) relationships can be inferred by analyzing genetic data from different plant species and are usually displayed as phylogenetic trees. Understanding phylogenetic relationships is important for identifying evolutionary patterns, predicting ecological and functional characteristics of plants, and guiding conservation efforts. Phylogenetics also provides insights into the evolution of traits, such as photosynthesis, growth, and development, as well as adaptations to different environmental conditions. Phylogenetic relationships among plant species have been investigated by analyzing genes coding for proteins, such as the oxygen-evolving complex (De Las Rivas & Roman, 2005), ATP synthase (Recipon *et al.*, 1992), and ferredoxin-$NADP^+$ reductase (Karlusich & Carrillo, 2017), which are directly involved in the generation, transport, and processing of protons during the light-dependent reactions of photosynthesis. Given that changes in enzyme structure and activity can impact isotope fractionation (Dirghangi & Pagani, 2013), species-related differences in genes coding for enzymes involved in photosystem II (Cameron *et al.*, 2006) may be one reason for the species-specific variations in the δ^2H_{ne} of primary assimilates and cellulose (Fig. 1).

To advance knowledge on species-specific drivers of ^2H fractionation, we conducted a comprehensive and systematic comparison across 152 Northern Hemisphere trees. As all sampled species grew in a common garden, impacts of climate and source water were neglectable. The selected trees represent 73 species, 48 genera, 19 families, and 12 orders containing both evergreen and deciduous angiosperms and gymnosperms, enabling us to test whether variation ^2H fractionation is driven by phylogenetic effects. We measured the $\delta^2H\delta$ of plant water (leaf water and twig xylem water) and $^2H_{ne}$ of carbohydrates (leaf sugars and twig xylem cellulose) using a recently developed hot water vapor equilibration technique for the δ^2H_{ne} analysis of plant carbohydrates (Schuler *et al.*, 2022). We tested the following hypotheses: (1) Phylogenetic distance is a major descriptor of the variation in ε_{HA} and ε_{HE}, translating to a clear phylogenetic pattern in the δ^2H_{ne} of leaf sugars and twig xylem cellulose. (2) The phylogenetic pattern decreases from sugars to cellulose, as the apparent ^2H fractionation in cellulose reflects more complex metabolic processes.

Materials and Methods

Site description

All tree and shrub species (Supporting Information Table S1) were growing in Kannenfeldpark in the city of Basel, Switzerland (0.91 km^2, 47°33′54.216″N, 7°34′16.126″E). The small sampling area, uniform site conditions, and flat surface minimize the variability in site conditions, and soil water isotopic signatures are uniform spatially. The mean annual temperature and mean annual precipitation sum for the site were 11.2°C and 841 mm, respectively, for the period 2000–2019 (IDAweb; MeteoSwiss, Zurich, Switzerland). Mean summer (June–August) temperature was 19.6°C, and mean summer precipitation was 263 mm over the same period. In the year of the sampling campaign (2019), the mean annual temperature was 11.6°C and precipitation summed to 786 mm. For the summer period of 2019, the mean temperature was 20.7°C and precipitation summed to 279 mm. The park is watered regularly during dry periods. Thus, it was assumed that trees and shrubs were not water limited in 2019 and that they used the same water source throughout the growing season.

Sampling of plant material

Leaves and twig material were sampled in summer 2019 from 73 species, 48 genera, 19 families and 12 orders, for a total of 152 trees (minimum of one tree per species; Table S1). Sampling was performed between 10:20 h and 16:00 h on 29 August and between 09:55 h and 13:00 h on 30 August to minimize the diel variability in the δ^2H of leaf water (Cernusak *et al.*, 2016). The two consecutive sampling days were sunny and warm, that is, 25.7–28.7°C (mean 26.6°C) and 51.3–60.7% relative humidity

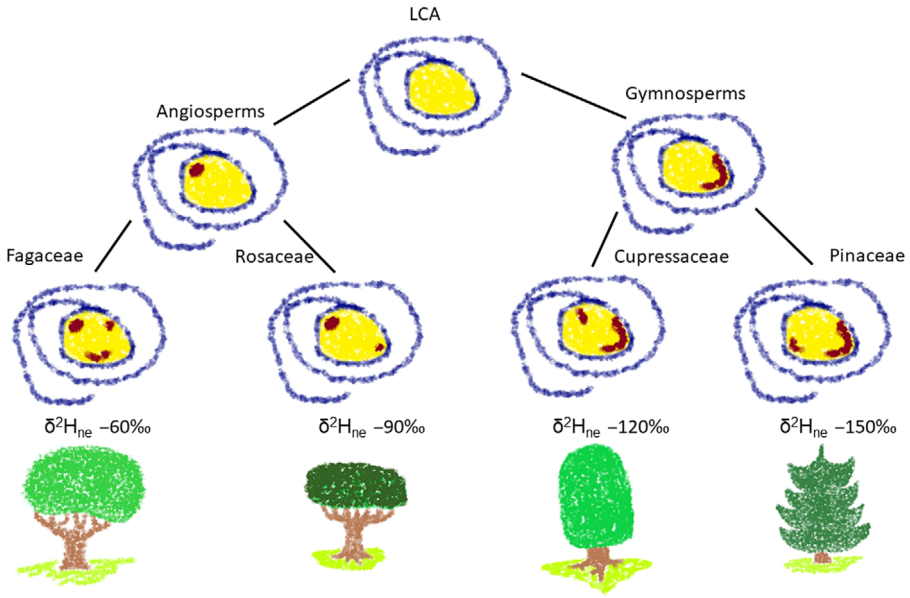

Fig. 1 Theoretical framework for the expected phylogenetic signal in the non-exchangeable hydrogen isotopic composition (δ^2H_{ne}) of carbohydrates in trees and shrubs. The last common ancestor (LCA) of all tested tree and shrub species had a hypothetical gene coding for a protein important in a distinct biological ^2H fractionation process during photosynthesis. The active region of the protein in the middle is shown in yellow. During the evolutionary separation between angiosperms and gymnosperms, certain genetic mutations lead to structural changes (red) of the active site of the protein, which was passed on to the next generations. During the evolution of the different tree families, additional small mutations occurred within both the angiosperm and gymnosperm families. The sum of all these small mutations has shaped the species-specific ^2H fractionation caused by the protein.

(mean 57.3%) on 29 August and 24.2–27.2°C (mean 25.9°C), and 55.0–70.5% (mean 62.8%) on 30 August (Table S2).

Branches were collected from sun-exposed canopies using pruners. The bark and phloem of *c.* 10 cm from the cut end of the twig samples were removed with a peeler. Whole, fully developed leaves and the separated twig xylem were immediately transferred into individual gas-tight 12-ml glass vials (Prod. No. 738 W, Exetainer; Labco, Lampeter, UK), stored on dry ice until the harvest was complete, and then stored in a −20°C freezer. For the extraction of the current-year twig xylem cellulose, twig material was transferred to paper bags, stored on dry ice, and then oven-dried for 72 h at 60°C.

Extraction of leaf and twig water, cellulose and sugars

Leaf water and twig water were cryogenically extracted using a hot water bath at 80°C and a vacuum (10^{-2} mbar) for 2 h (West *et al.*, 2006; Diao *et al.*, 2022), then stored in glass vials at −20°C until δ^2H measurement. The dried leaf material from the cryogenic vacuum distillation was ball-milled (MM400; Retsch, Haan, Germany), and the bulk leaf sugar fraction (i.e. 'leaf sugars') was then extracted from 100 mg of leaf powder following established protocols for carbon and oxygen isotope analysis (Rinne *et al.*, 2012; Lehmann *et al.*, 2020). First, the ground leaf material was mixed with deionized water in a 2-ml reaction vial and the water-soluble content was extracted at 85°C for 30 min. Leaf sugars were then purified from the water-soluble content using ion exchange cartridges (OnGuard II A, H and P, Dionex; Thermo Fisher Scientific, Bremen, Germany). The remaining sugar solutions were frozen and freeze-dried, and the mass of each sugar sample was measured.

For the extraction of twig xylem holocellulose, the twig xylem tissue from the current year was visually identified, separated manually with scissors, and ball-milled to a powder (Retsch). About 100 mg of the ball-milled material was packed into F57 fiber filter bags (Ankom Technology, Macedon, NY, USA). The samples were washed twice, for 2 h each time, with 5% NaOH at 60°C. The samples were then rinsed three times with boiling deionized water and subsequently incubated three times at 60°C, for 8 h each time, in a solution of 7% $NaClO_2$ adjusted with 96% acetic acid to a pH of 4–5. After that, the samples were again rinsed three times with boiling deionized water, squeezed using a spatula, and dried for at least 4 h in a drying oven at 60°C. In a final step, the purified cellulose was mixed with deionized water, homogenized with an ultrasonic transducer (UP200St; Hielscher, Teltow, Germany), and freeze-dried overnight.

δ^2H analysis of twig xylem water (δ^2H_{XW}) and leaf water (δ^2H_{LW})

The δ^2H of water samples was measured with a high-temperature conversion elemental analyzer coupled to a DeltaPlus XP isotope ratio mass spectrometer (TC/EA-IRMS; Finnigan MAT, Bremen, Germany). Calibration was performed using a range of certified waters of different isotope δ^2H ratios, resulting in a precision of analysis of 2‰.

δ^2H_{ne} analyses of sugars and cellulose using a hot water vapor equilibration method

For the δ^2H_{ne} analyses of sugars and cellulose, the previously developed hot water vapor equilibration method was applied (Schuler *et al.*, 2022). In short, the dried sugar samples were dissolved in water, with a target concentration of 1 mg per 20 µl. The reason for this relatively high target was to reduce sample volume and increase its viscosity, thereby reducing the risk of losing sample material while processing. Two identical sets of each sugar sample, with 1 mg sample material each, were prepared by pipetting 20 µl into preweighed 5 × 9 mm silver foil capsules (SA76981106; Säntis, Rüthi, Switzerland). Each duplicate was then frozen at −20°C, freeze-dried at −50°C, and packed into a second silver foil capsule to prevent sample loss during the equilibration process

when sugars are liquified. Cellulose samples were also prepared in duplicate by transferring 1 mg into 3.3 × 5 mm silver foil capsules (SA76980506; Säntis, Rüthi, Switzerland). Sugar and cellulose samples were stored in a desiccator at low relative humidity (2–5%) until δ^2H measurement.

The two sets of duplicates were then equilibrated with water vapor using two isotopically distinct waters (δ^2H (Water 1) = −160‰ and δ^2H (Water 2) = −428‰) at 130°C in an apparatus consisting of an electrical heating oven (ED23; Binder, Tuttlingen, Germany) into which a specially designed equilibration chamber was inserted (Schuler *et al.*, 2022). After 2 h of equilibration with hot water vapor, the continuous water flow was stopped, the excess water in the line was pumped back and discarded, the feeding capillary was switched to a capillary delivering dry nitrogen gas (N25.0; 2220912; PanGas AG, Dagmersellen, Switzerland) for 2 h to remove any remaining water and water vapor from within the equilibration chamber. The system remained at 130°C during the drying time. After the samples were equilibrated and dried, they were immediately transferred into a Zero Blank Autosampler (N.C. Technologies Srl, Milano, Italy), which was installed on a sample port of a high-temperature elemental analyzer system. The latter was coupled via a ConFlo III referencing interface to a Delta^{Plus} XP IRMS (TC/EA-IRMS; Finnigan MAT, Bremen, Germany). The autosampler was evacuated to 0.01 mbar and filled with dry helium gas to avoid exchange of H_{ex} with ambient water vapor. The samples were pyrolyzed in a reactor according to Gehre *et al.* (2004), and carried in a flow of dry helium (150 ml min^{-1}) to the IRMS. Raw δ^2H values were offset corrected using PEF standards (IAEA-CH-7 polyethylene foil, International Atomic Energy Agency, Vienna, Austria; SD < 0.7‰ within one run). The measured δ^2H of the leaf sugar and twig xylem cellulose can be found in Tables S3 and S4, respectively.

Calculation of the nonexchangeable hydrogen isotope ratio (δ^2H_{ne}), ε_{HA} and ε_{HE}

All Isotope ratios (δ) were calculated as given in Eqn 1 (Coplen, 2011):

$$\delta = \frac{R_{Sample} - R_{Standard}}{R_{Standard}} \quad \text{Eqn 1}$$

where $R = {}^2H/{}^1H$ of the sample (R_{Sample}) and of Vienna Standard Mean Ocean Water (VSMOW2; $R_{Standard}$) as the standard defining the international isotope scale. To express the resulting δ in permil (‰), results were multiplied by 1000.

According to Filot *et al.* (2006), the %-proportion of exchanged hydrogen during the equilibrations (x_e, Eqn 2) can be calculated as:

$$x_e = \frac{\delta^2H_{e1} - \delta^2H_{e2}}{\alpha_{e-w} \cdot (\delta^2H_{w1} - \delta^2H_{w2})} \quad \text{Eqn 2}$$

where δ^2H_{e1} and δ^2H_{e2} are the measured δ^2H values of the two equilibrated subsamples, δ^2H_{w1} and δ^2H_{w2} are the δ^2H values of the two waters used, and α_{e-w} is the fractionation factor of 1.082, which is the same for sugars and cellulose (Filot *et al.*, 2006; Schuler *et al.*, 2022). Typical x_e values for sugars are between 0.32 and 0.36, and for cellulose *c.* 0.20 (Schuler *et al.*, 2022).

δ^2H_{ne} can then be calculated with Eqn 3 using one of the two equilibrations (equilibration one in this example, δ^2H_{e1} and δ^2H_{w1}):

$$\delta^2H_{ne} = \frac{\delta^2H_{e1} - x_e \cdot \alpha_{e-w} \cdot \delta^2H_{w1} - 1000 \cdot x_e \cdot (\alpha_{e-w} - 1)}{1 - x_e} \quad \text{Eqn 3}$$

The results were then calibrated using internal reference material, with three sucrose samples for the equilibrations of leaf sugars and three cellulose samples for the equilibrations of the twig xylem cellulose. The calculation of the δ^2H_{ne} of the leaf sugar and twig xylem cellulose can be found in Tables S3 and S4, respectively.

The total leaf water enrichment (LWE) was calculated with Eqn 4, ε_{HA} with Eqn 5, and ε_{HE} with Eqn 6, using the values for leaf water (δ^2H_{LW}) and xylem water (δ^2H_{XW}):

$$LWE = \delta^2H_{leaf\ water} - \delta^2H_{twig\ xylem\ water} \quad \text{Eqn 4}$$

$$\varepsilon_{HA} = \delta^2H_{leaf\ sugar} - \delta^2H_{leaf\ water} \quad \text{Eqn 5}$$

$$\varepsilon_{HE} = \delta^2H_{twig\ xylem\ cellulose} - \delta^2H_{leaf\ sugar} \quad \text{Eqn 6}$$

To eliminate unnecessary complexity, in agreement with the law of parsimony in explaining observed processes, the two biological fractionation factors were expressed as the actual difference between the δ^2H_{ne} of leaf sugars and the δ^2H of leaf water (ε_{HA}), and the actual difference between the δ^2H_{ne} of twig xylem cellulose and the δ^2H of leaf sugars (ε_{HE}).

Statistical analyses

Statistical analyses were performed using R v.4.1.2 (R Core Team, 2021). The distribution of the data was assessed for normality with Kolmogorov–Smirnov tests. *T*-tests were performed to evaluate δ^2H fractionation differences between angiosperms and gymnosperms, as well as between deciduous and evergreen species. Analysis of variance (ANOVA), followed by Tukey's *post hoc* tests, was performed to evaluate differences between clades, orders, families, and genera. Linear models, implemented in the R package GGPLOT2 (Wickham, 2016), were used to determine the general drivers behind the ^2H fractionation processes. Final assembly of the graphs was done using the R package PATCHWORK (Pedersen, 2022). The phylogenetic analyses were performed and the phylogenetic trees were generated using the R package PHYTOOLS (Revell, 2012). Pagel's λ was used to estimate the phylogenetic signal behind the observed δ^2H_{ne} of leaf sugars and twig xylem cellulose and the fractionation factors (ε_{HA} and ε_{HE}). According to Molina-Venegas & Rodríguez (2017), Pagel's λ measures the similarity of the covariances among species and the covariances expected for values with a distribution similar to

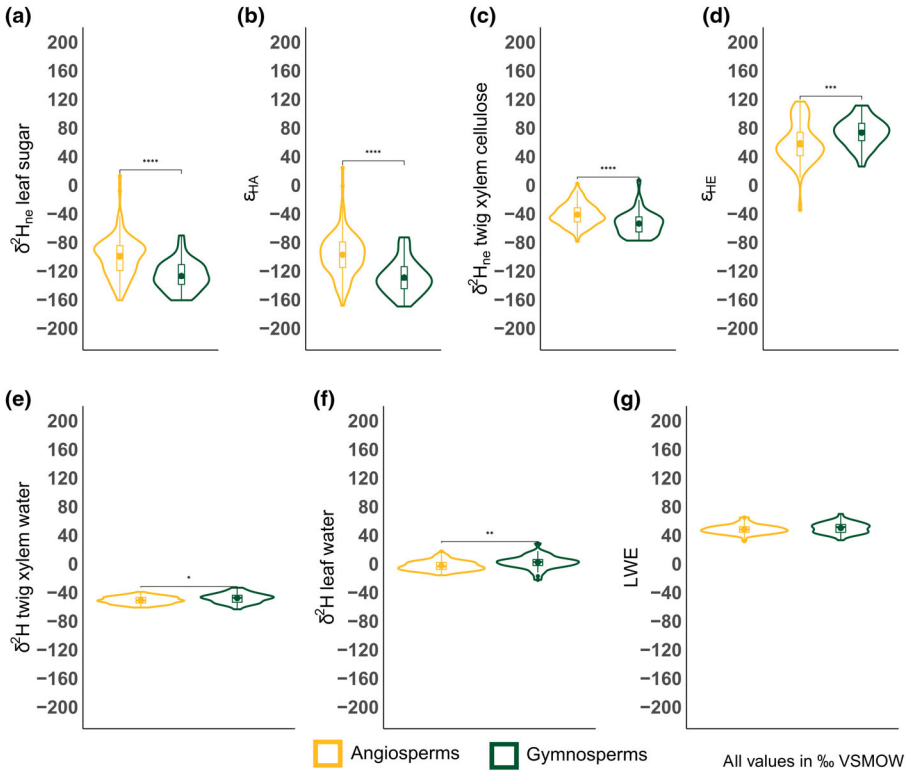

Fig. 2 Violin plots of the hydrogen (H) isotope ratios of plant water and carbohydrates and their ^{2}H fractionation factors across 152 tree and shrub species in a common garden. The boxplots within the violin plots are indicating the mean (points) and median (horizontal line) values. (a) Non-exchangeable H isotopic composition (δ^2H_{ne}) of leaf sugar, (b) autotrophic ^{2}H fractionation factor (ε_{HA}), (c) δ^2H_{ne} of twig xylem cellulose, (d) heterotrophic ^{2}H fractionation factor (ε_{HE}), (e) δ^2H of twig xylem water, (f) δ^2H of leaf water, and (g) leaf water enrichment (LWE). In all panels, angiosperms (yellow) and gymnosperms (green) are compared, with asterisks indicating significant differences (*t*-test: *, $P \leq 0.05$; **, $P \leq 0.01$; ***, $P \leq 0.001$; ****, $P \leq 0.0001$). VSMOW, Vienna Standard Mean Ocean Water.

Brownian motion. It is highly robust to incompletely resolved phylogenies and suboptimal branch-length information. A Pagel's λ of 1 indicates a strong phylogenetic signal, where the tested trait is more similar in closely related species than in more distantly related species. By contrast, a Pagel's λ of 0 indicates the absence of a phylogenetic signal, which means that the variability of the tested trait is not affected by the evolutionary relationships of the species. As there was no calibrated phylogenetic tree available containing all the considered species, generic branch lengths were used for the phylogenetic tree: 1 on the species level, 2 on the genus level, 4 on the family level, 8 on the order level, and 16 between angiosperms and gymnosperms. This was done with the aim of reflecting the increasing phylogenetic distance along this sequence. Due to the uneven number of replicates (one to three) within the tested species, mean values per species were used.

Results

δ^2H of plant water and carbohydrates in angiosperms and gymnosperms

The measured δ^2H and ^{2}H fractionation factors of carbohydrates and water in angiosperms and gymnosperms were normally distributed (Fig. 2a–d), with mostly unimodal peaks around the mean values, and the mean and median values close to each other. For the ε_{HE} of angiosperms, there was a slightly bimodal but still normal distribution (Fig. 2d), with a secondary accumulation at values about twice as large as the bulk of the ε_{HE} values.

Among the sampled species and phylogenetic groups (clade, order, family, genus, species), we observed large variability in the δ^2H_{ne} of leaf sugars and twig xylem cellulose and in the biological fractionation factors ε_{HA} and ε_{HE} (Fig. 2; Tables 1, S1, S5, S6). For angiosperm carbohydrates, the mean δ^2H_{ne} values of leaf sugars and twig xylem cellulose were −99.9‰ (SD = 28.1‰) and −41.2‰ (SD = 15.2‰), respectively. The observed δ^2H in angiosperms resulted in mean ε_{HA} and ε_{HE} values of −97.3‰ (SD = 30.5‰) and 58.7‰ (SD = 28.3‰), respectively. For gymnosperm carbohydrates, the mean δ^2H_{ne} values of leaf sugars and twig xylem cellulose were −127.0‰ (SD = 20.5‰) and −53.7‰ (SD = 16.9‰), respectively. The observed δ^2H in gymnosperms resulted in mean ε_{HA} and ε_{HE} values of −129.1‰ (SD = 23.4‰) and 73.2‰ (SD = 19.6‰), respectively. The ε_{HA} values of gymnosperm species were significantly lower than those of angiosperm species ($P \leq 0.0001$), whereas ε_{HE} values were significantly higher for gymnosperms ($P \leq 0.001$).

In comparison with the δ^2H_{ne} of sugars and cellulose (Fig. 2a–d), variability was smaller for δ^2H_{XW}, δ^2H_{LW}, and LWE (Fig. 2e–g). In angiosperms, the mean δ^2H values of twig xylem water and leaf water were −50.8‰ (SD = 5.0‰) and −2.6‰ (SD = 6.7‰), respectively, leading to a mean isotopic leaf water enrichment (LWE) of 48.2‰ (SD = 6.1‰; Fig. 2). In gymnosperms, the mean δ^2H values of twig xylem water and leaf water were −47.9‰ (SD = 6.7‰) and 2.1‰ (SD = 9.4‰), respectively, leading to a mean isotopic leaf water enrichment of 50.2‰ (SD = 7.5‰; Fig. 2). The δ^2H values of xylem and leaf water were significantly higher in gymnosperms than in angiosperms ($P \leq 0.05$), while LWE was not significantly different between the two groups ($P \geq 0.05$).

Within the tested angiosperms, *Ilex aquifolium* L. had the smallest ε_{HA}, with a mean of −7.1‰ (SD = 34.7‰), leading to

Table 1 Order-level mean values and standard deviations (SD) of δ^2H_{ne} of plant carbohydrates, ε_{HA} and ε_{HE}, δ^2H of twig xylem water and leaf water, and leaf water enrichment (LWE).

		δ^2H_{ne} leaf sugar (‰)			ε_{HA} (‰)			δ^2H_{ne} xylem cellulose (‰)			ε_{HE} (‰)			δ^2H twig xylem water (‰)			δ^2H leaf water (‰)			Leaf water enrichment (‰)		
Order	*n*	Mean	SD	Group	Mean	SD	Group	Mean	SD	Group	Mean	SD	Group	Mean	SD	Group	Mean	SD	Group	Mean	SD	Group
Aquifoliales	3	−15.1	31.7	A	−7.12	34.7	A	−24.3	11.2	ABC	−9.2	38.6	D	−47.7	3.7	AB	−8.0	3.3	AB	39.7	5.6	B
Buxales	3	−95.3	4.56	BCDE	−101	2.3	BCD	−43.9	4.3	ABC	51.4	8.7	ABCD	−44.0	2.1	AB	5.3	4.0	AB	49.2	5.0	AB
Fabales	5	−134	30.4	DE	−137	34.9	D	−45.2	14.9	BC	88.9	29.3	A	−54.8	4.4	AB	3.3	10.2	AB	58.1	6.9	A
Fagales	47	−100	18.3	C	−99	18.5	C	−46.8	14.0	BC	53.3	19.9	BC	−49.4	5.5	AB	−1.2	5.7	AB	48.2	5.0	B
Lamiales	9	−72.7	25.3	B	−65.5	28.6	B	−16.2	11.4	A	56.6	27.4	ABC	−50.9	3.7	AB	−7.3	5.3	B	43.7	5.9	B
Magnoliales	13	−116	25.2	CDE	−114	27	CD	−40.0	10.3	BC	75.5	27.2	AB	−49.9	2.6	AB	−1.2	6.5	AB	48.7	5.8	AB
Malvales	5	−82.6	3.98	BC	−77.6	6.7	BC	−46.8	5.8	BC	35.8	6.6	CD	−53.8	3.6	AB	−4.9	5.9	AB	48.9	4.6	AB
Rosales	13	−102	25.3	BCDE	−94.7	27	BC	−41.8	12.7	BC	59.8	31.0	ABC	−52.8	4.4	AB	−6.9	5.5	B	45.9	4.8	B
Sapindales	12	−117	16.2	CDE	−113	19.9	CD	−39.9	13.7	BC	77.2	24.2	AB	−55.0	3.4	B	−4.5	7.5	AB	50.6	6.7	AB
Saxifragales	1	−86.6	NA	ABCDE	−91.4	NA	ABCD	−23.0	NA	ABC	63.6	NA	ABCD	−47.3	NA	AB	4.8	NA	AB	52.1	NA	AB
Ginkgoales	2	−96.2	36.5	BCDE	−96.4	33	BCD	−52.1	10.9	ABC	44.1	25.6	ABCD	−50.9	4.7	AB	0.2	3.5	AB	51.0	8.2	AB
Pinales	39	−129	18.8	E	−131	22.1	D	−53.8	17.2	C	74.7	18.4	A	−47.7	6.8	A	2.2	9.6	A	50.0	7.6	AB

The corresponding grouping according to the analysis of variance and Tukey's *post hoc* tests is shown.

a mean δ^2H_{ne} of leaf sugars of −15.1‰ (SD = 31.7‰). Interestingly, this species was the only one with a negative heterotrophic ^2H fractionation factor ε_{HE} (mean = −9.2‰, SD = 38.6‰), leading to a mean δ^2H_{ne} of twig xylem cellulose of −24.3‰ (SD = 11.2‰). While gymnosperms showed, on average, a stronger ^2H fractionation than angiosperms, the order with the strongest ^2H fractionation, for both ε_{HA} and ε_{HE}, was the angiosperm Fabales (ε_{HA} mean −137.4‰, SD = 34.9‰; ε_{HE} mean 88.9‰, SD = 29.3‰). We observed no significant differences for the tested variables (δ^2H_{ne} of leaf sugar, ε_{HA}, δ^2H_{ne} of twig xylem cellulose, ε_{HE}, δ^2H of twig xylem water, δ^2H of leaf water, and LWE) between the deciduous and evergreen species within the angiosperms and within the gymnosperms ($P > 0.05$, Fig. S1).

Relationship between δ^2H of plant water and carbohydrates

δ^2H_{ne} of leaf sugars was not or only very weakly ($R^2 < 0.1$) linearly related to δ^2H of twig xylem water and of leaf water and to LWE (Fig. 3a–c), but it was strongly linearly related to ε_{HA} ($R^2 = 0.95$; Fig. 3d) and to ε_{HE} ($R^2 = 0.68$; Fig. 3e). For δ^2H_{ne} of twig xylem cellulose, we observed a weak relationship ($R^2 = 0.1$) with δ^2H of twig xylem water (Fig. 4a), but no or very weak relationships with δ^2H of leaf water and with LWE (Fig. 4b,c). In contrast to values for leaf sugars, δ^2H_{ne} of twig xylem cellulose was only weakly related to ε_{HA} ($R^2 = 0.16$; Fig. 4d) and to ε_{HE} ($R^2 = 0.19$; Fig. 4e).

Phylogenetic analysis of the observed δ^2H patterns

Pagel's λ, a measure of phylogenetic effects, differed among the isotopic variables (Table 2; Figs S2–S4). For δ^2H_{ne} of leaf sugars and for ε_{HA}, Pagel's λ values were close to 1, indicating a clear phylogenetic signal. Similarly, a phylogenetic signal was visible in the δ^2H_{ne} of twig xylem cellulose and in ε_{HE}, albeit weaker. No significant phylogenetic signal was observed in the δ^2H of xylem water, leaf water, or LWE (Table 2).

The phylogenetic trees for δ^2H_{ne} of the carbohydrates and the corresponding fractionation factors (Figs 5, 6), in combination with the ANOVA results (Table S6), indicated distinct patterns among the tested phylogenetic groups. The phylogenetic tree for δ^2H_{ne} of leaf sugars (Fig. 5a) showed lower (more negative) δ^2H_{ne} values for gymnosperms than for angiosperms. Three groups of angiosperms had lower δ^2H_{ne} of leaf sugars compared with the other angiosperms: the family Fabaceae, the genus *Acer* L., and, to a lesser extent, the family Magnoliaceae. The phylogenetic pattern of ε_{HA} reflected the phylogenetic relationships of the δ^2H_{ne} of leaf sugars (Fig. 5b), demonstrating that leaf water did not shape the detected phylogenetic pattern. Within the gymnosperms, there were no significant differences for δ^2H_{ne} of leaf sugars and ε_{HA}, whereas the ε_{HA} of Ginkgoaceae and Taxaceae were significantly different than the values for Cupressaceae and Pinaceae (Table S6).

The phylogenetic tree for δ^2H_{ne} of twig xylem cellulose (Fig. 6a) revealed a different and slightly more complex pattern than observed for the δ^2H_{ne} of leaf sugars and for ε_{HA}. While δ^2H_{ne} values were, on average, lower (more negative) in

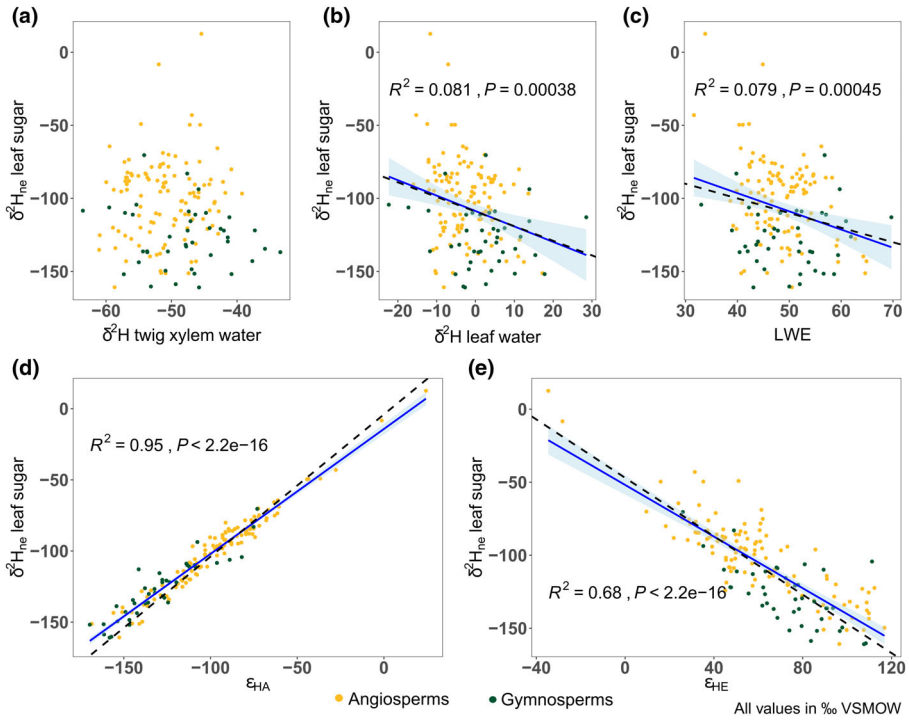

Fig. 3 Linear relationships between δ^2H_{ne} of leaf sugars and (a) δ^2H of twig xylem water, (b) δ^2H of leaf water, (c) leaf water enrichment (LWE), (d) autotrophic ^2H fractionation factor (ε_{HA}), and (e) heterotrophic ^2H fractionation factor (ε_{HE}). Yellow dots indicate angiosperms, and green dots indicate gymnosperms. The continuous blue line represents the linear model, the light blue shading denotes the 95% confidence level interval for predictions from the linear model, and the dashed black line is the 1 : 1 line. VSMOW, Vienna Standard Mean Ocean Water.

gymnosperms than in angiosperms, we found distinct groups within both angiosperms and gymnosperms. For angiosperms, there were three distinct groups: species of the family Fagaceae (containing *Betula* L., *Alnus* MILL., *Carpinus* L. and *Ostrya* SCOP.) had the lowest δ^2H_{ne} of twig xylem cellulose; species within the genus *Fraxinus* L. had the highest δ^2H_{ne} values; and the remaining species had δ^2H_{ne} values distributed between those of the two other groups. For gymnosperms, species within the family Pinaceae had higher δ^2H_{ne} of twig xylem cellulose than observed for species belonging to the families Cupressaceae and Taxaceae.

For the phylogenetic tree of ε_{HE} (Fig. 6b), angiosperm species were divided into three different groups. Species of the family Fabaceae and the genus *Acer* were distinguished by a stronger ^2H enrichment, caused by ε_{HE}, compared with the other angiosperms. Interestingly, *Ilex aquifolium* was the only species with a negative ε_{HE}, leading to a ^2H depletion from leaf sugars to xylem cellulose. As with ε_{HA}, for ε_{HE} two distinct groups within the gymnosperms were observed (Fig. 6b; Table S6): species within the family Pinaceae, where ε_{HE} caused a strong ^2H enrichment, and species of the families Cupressaceae, Taxaceae, and Ginkgoaceae, with much lower ε_{HE} values.

Discussion

Phylogenetic pattern in the δ^2H_{ne} of plant carbohydrates, ε_{HA} and ε_{HE}

Our study revealed a strong phylogenetic signal in the hydrogen isotopic composition of plant carbohydrates (Tables 1, 2; Figs 5, 6, S2, S3). Given that δ^2H in twig xylem and leaf water varied less and that species-related trends in plant water were opposite to those in carbohydrates (Figs 2, 3), we conclude that the phylogenetic signal in the δ^2H_{ne} of plant carbohydrates was not driven by source or leaf water (Figs 3, 4), which is in accordance with recent studies (Holloway-Phillips *et al.*, 2022). A strong relationship between the δ^2H of the source water and the δ^2H_{ne} of carbohydrates probably only occurs if plants are growing with source water with pronounced differences in their δ^2H, such as along a geographic gradient along a dividing range (Roden & Ehleringer, 2000), on the continental scale (West *et al.*, 2008; Vitali *et al.*, 2022), or when source water is experimentally enriched or depleted in ^2H (Roden & Ehleringer, 1999). Instead, our results showed that the δ^2H_{ne} of sugars and cellulose and their phylogenetic signal were caused by biological processes, and differed between angiosperms and gymnosperms (Fig. 2). ε_{HA} explained 95% of the variation in the δ^2H_{ne} of leaf sugars. The strong relationship between these two variables (Fig. 2d) indicates that the observed δ^2H_{ne} of leaf sugars was representative for the sampled species.

The strong phylogenetic pattern of the δ^2H_{ne} of leaf sugars and ε_{HA} was dampened during heterotrophic ^2H fractionation (ε_{HE}), as the isotopic signal in leaf sugars was not directly translated into twig xylem cellulose (Figs 3, 4), resulting in a reduced phylogenetic pattern in δ^2H_{ne} of twig xylem cellulose (Figs 6, S3; Table 2). The change in ^2H signal transfer from leaf sugars to cellulose might also be partially explained by a temporal and spatial separation between ^2H fractionation processes shaping the δ^2H_{ne} of leaf sugars and those shaping the δ^2H_{ne} of twig xylem cellulose. By contrast, drivers of heterotrophic ^2H fractionation and the δ^2H_{ne} of twig xylem cellulose were likely more complex than those influencing ε_{HA}. These heterotrophic ^2H fractionation processes might be influenced by the physiological adaption of a species to its environment, such as the interaction of respiration rate

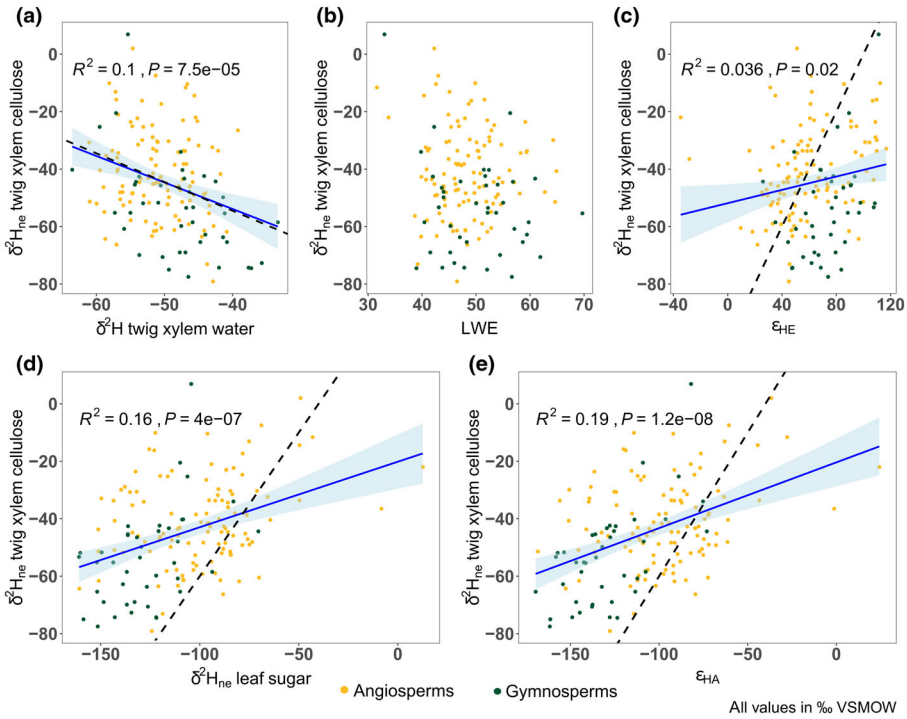

Fig. 4 Linear relationship between δ^2H_{ne} of twig xylem cellulose and (a) δ^2H of twig xylem water, (b) leaf water enrichment (LWE), (c) heterotrophic ^2H fractionation factor (ε_{HE}), (d) δ^2H_{ne} of leaf sugars, and (e) autotrophic ^2H fractionation factor (ε_{HA}). Yellow dots indicate angiosperms, and green dots indicate gymnosperms. The continuous blue line represents the linear model, the light blue shading denotes the 95% confidence level interval for predictions from the linear model, and the dashed black line is the 1 : 1 line. VSMOW, Vienna Standard Mean Ocean Water.

Table 2 Pagel's λ for δ^2H of plant water (leaf water, twig xylem water), δ^2H_{ne} of plant carbohydrates (leaf sugars, twig xylem cellulose), leaf water enrichment (LWE), and the autotrophic (ε_{HA}) and heterotrophic (ε_{HE}) ^2H fractionation factors.

	Pagel's λ	*P*
δ^2H_{ne} leaf sugar	0.87	***
ε_{HA}	0.88	***
δ^2H_{ne} twig xylem cellulose	0.64	***
ε_{HE}	0.61	***
δ^2H twig xylem water	0.26	ns
δ^2H leaf water	0.03	ns
LWE	0	ns

with temperature (Patterson *et al.*, 2018), or by differences in tree internal carbon allocation (Herrera-Ramírez *et al.*, 2020).

An evolutionary development causing the stronger autotrophic ^2H fractionation in gymnosperms could be their faster electron transport of photosystem II compared with angiosperms (Shirao *et al.*, 2013), which might also affect the rate of proton transport, leading to stronger ^2H fractionation. Other known differences between gymnosperms and angiosperms are the higher water use efficiency of the former (Flexas & Carriquí, 2020), as well as differences in their leaf hydraulics and stomatal conductance (Lusk *et al.*, 2003; Brodribb *et al.*, 2005). However, these variables would explain the observed pattern in ^2H fractionation only if the ^2H fractionation were derived from the leaf water, which was not the case in our study (Figs 3, 4). The absence of any relationship between the δ^2H of leaf water and the δ^2H_{ne} of carbohydrates might be caused by strong isotopic differences between the water of the whole leaf and the water inside the chloroplasts, which is the isotopically relevant pool during C_3 carbon fixation, due to the photosynthetic proton production inside the chloroplast (Heldt *et al.*, 1973). In this case, the δ^2H of the water inside the plants' chloroplasts might be responsible for the phylogenetic relationships detected here. Relationships in the H isotopic signal in leaf and source water and carbohydrates, reported by others (Roden & Ehleringer, 2000), would only occur if plants of the same species grew with source water with different δ^2H values. Nitrogen metabolism is a process that could influence ε_{HE}, as gymnosperms have a lower photosynthetic nitrogen use efficiency than angiosperms (Flexas & Carriquí, 2020). However, the nitrogen metabolism of the tree and shrub species considered here probably did not contribute significantly and consistently to the observed phylogenetic pattern in plants' ^2H fractionation, as the nitrogen-fixing angiosperm species within Fabales and the two *Alnus* species within Fagales had different patterns of autotrophic and heterotrophic ^2H fractionation (Tables S5, S6).

Another potential reason for the difference between our tested angiosperm (mostly deciduous) and gymnosperm (mostly evergreen) species could be related to findings from recent studies showing a ^2H depletion in tree-ring cellulose of deciduous compared with evergreen conifer species (Arosio *et al.*, 2020a,b), suggesting an influence of leaf shedding behavior. However, in our data set, which included more species from more genera than previous studies, such differences did not emerge between deciduous and evergreen species for either angiosperms or gymnosperms (Fig. S1). This was the case even when we reduced our data set to the species used by Arosio *et al.* (2020b).

One reason for the differences between our findings and those from previous studies could be related to the plant tissue

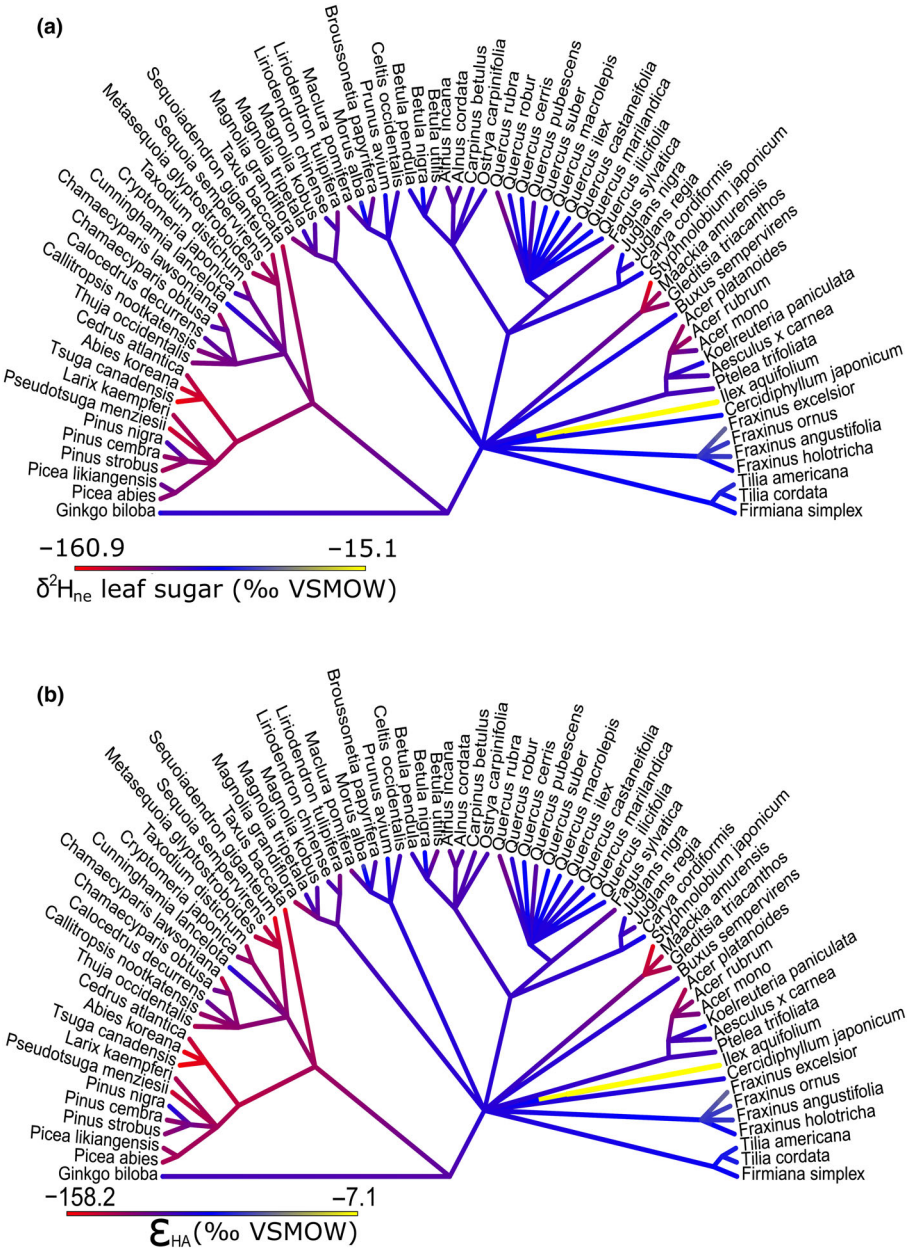

Fig. 5 Phylogenetic trees showing (a) the δ^2H_{ne} of leaf sugars and (b) the autotrophic ^2H fractionation factor between leaf water and leaf sugars (ε_{HA}) among the tested tree species. Gymnosperms are on the left side and angiosperms on the right side of the tree. VSMOW, Vienna Standard Mean Ocean Water.

analysed. While we used current-year twig material for the cellulose extraction, cellulose derived from branch material was investigated in earlier studies. δ^2H_{ne} of twig xylem cellulose from current-year twigs should reflect nearly exclusively stable isotope ratios of fresh assimilates, as the NSC pool in the canopy is largely depleted during leaf flushing (Nabeshima *et al.*, 2018; Palacio *et al.*, 2018; Tixier *et al.*, 2018). By contrast, cellulose synthesis in older branch and stem tissues might use a larger percentage of older carbon reserves, which might be isotopically distinct from fresh NSCs due to heterotrophic fractionations, isotopic mixing, and the integration of larger temporal variations, for example, in climate. The overall composition of the NSC storage pools of deciduous and evergreen species might also differ in terms of the time of the year when these assimilates were formed. Unlike deciduous species, evergreen species can assimilate throughout the entire year if the climatic conditions are favorable (Hadley, 2000; Schaberg, 2000; Zhang *et al.*, 2013) and may use isotopically different water sources in different seasons. This might lead to distinct differences in the δ^2H of assimilates during summer and winter.

Therefore, the phylogenetic signals in the δ^2H_{ne} of leaf sugars might be overwritten along the path to tree-ring cellulose by other physiological and phenological traits. This possibility needs to be investigated in further studies. Thus, we conclude that any differences in δ^2H between deciduous and evergreen tree species under the same climatic conditions, apart from the species specific pattern in ^2H fractionation, were probably tissue specific and caused by the use of different proportions of fresh and old NSCs and by temporal variation in their photosynthetically active period.

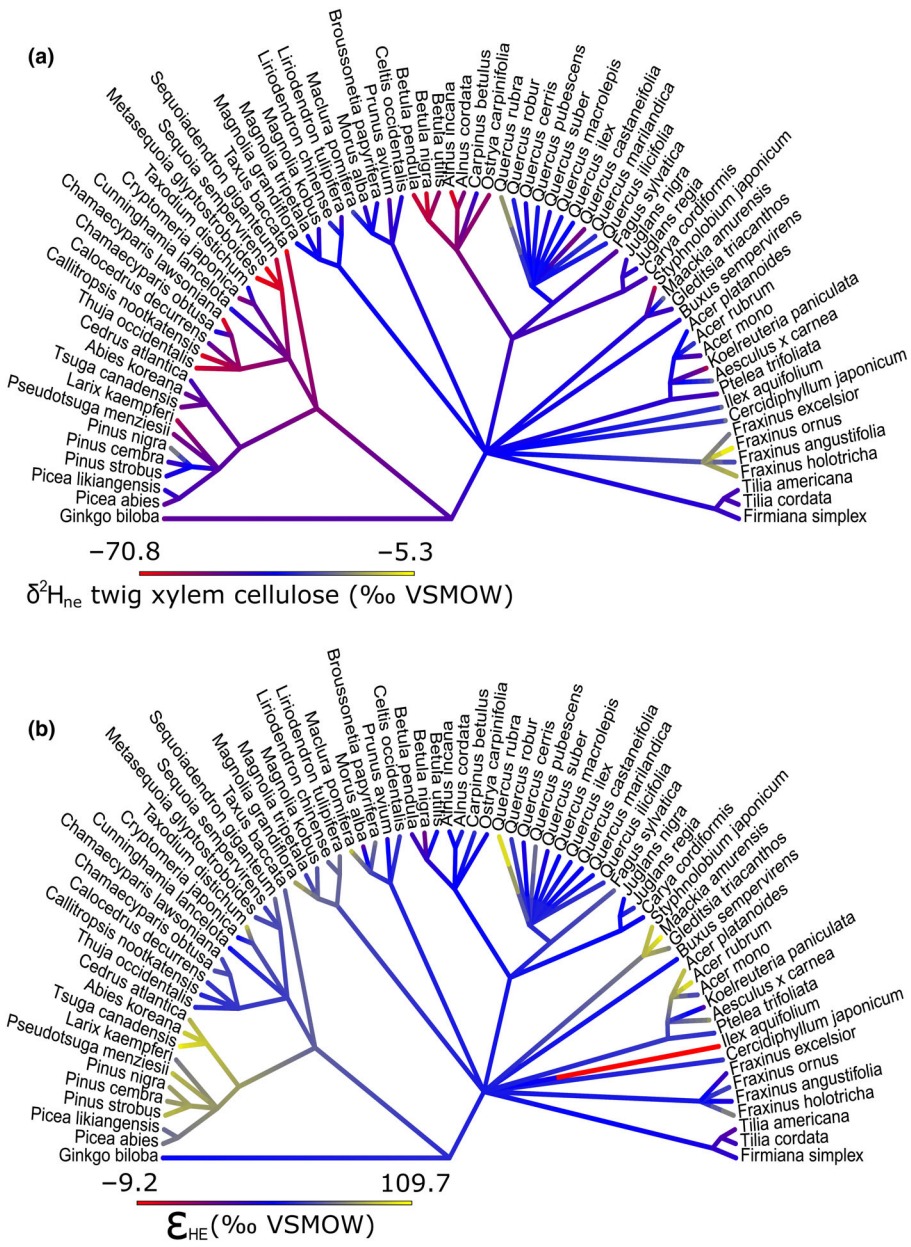

Fig. 6 Phylogenetic trees showing (a) the δ^2H_{ne} of twig xylem cellulose and (b) the heterotrophic ^2H fractionation factor between leaf sugars and twig xylem cellulose (ε_{HE}) among the tested tree species. Gymnosperms are on the left side and angiosperms on the right side of the tree. VSMOW, Vienna Standard Mean Ocean Water.

Potential drivers of autotrophic and heterotrophic ^2H fractionation

Our results suggested that δ^2H_{ne} was driven by autotrophic ^2H fractionation, as leaf water could be ruled out as an important driver of the δ^2H_{ne} of carbohydrates (Figs 2, 3a,b, 4a,b; Tables 1, 2). A closer look at the biochemical reactions inside the chloroplast with the potential to impact the δ^2H_{ne} of freshly assimilated sugars might narrow down the processes that could cause the observed phylogenetic signal in the ^2H fractionation (ε_{HA}) in the leaf sugars of tree and shrub species (Fig. 7).

Photosynthetic carbon (C) fixation is divided into light-dependent (Fig. 7a) and light-independent reactions (Fig. 7b). During the light-dependent reactions (Fig. 7a), H^+ is produced inside the thylakoid lumen (Ferreira *et al.*, 2004) and subsequently transported through the thylakoid membrane into the chloroplast stroma. There, H^+ is used to synthetize NADPH (Nelson & Ben-Shem, 2005). H^+ undergoes continuous exchange reactions with the H of the H_2O (Giguere, 1979), both inside the water pool of the thylakoid lumen and in the chloroplast stroma, causing an additional potential for ^2H fractionation, as relative energies of ^1H and ^2H bonds are affected by their differences in zero-point vibrational energy (Scheiner & Čuma, 1996). These light-dependent reactions produce a strong H^+ gradient between the thylakoid lumen and the chloroplast stroma, leading to a ΔpH of 2.3 between the two compartments (Heldt *et al.*, 1973; Falkner *et al.*, 1976; Heldt, 1980). New sugars are synthetized during the light-independent reactions (Fig. 7b). These sugars have seven C-bound H atoms, which can originate from the NADPH pool (21%), from photorespiration

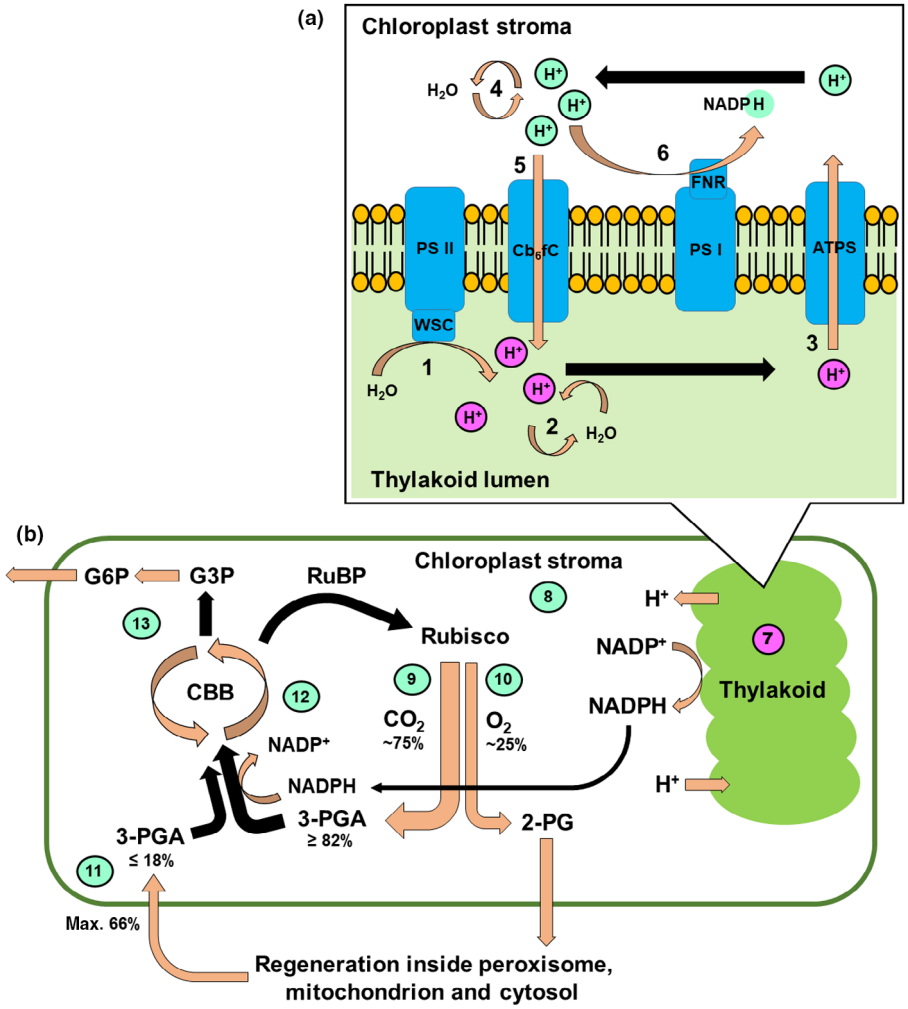

Fig. 7 Simplified scheme of photosynthesis, showing only the steps where hydrogen (H, i.e. protons) is directly involved: (a) light-dependent reactions in the thylakoid according to Allen *et al*. (2011), and (b) light-independent reactions in the chloroplasts' stroma according to Busch (2020). Bold numbers indicate reactions where strong ^{2}H fractionation is likely to occur. The proton pool within the thylakoid lumen is shown as pink circles, while the proton pool in the chloroplast stroma is shown as mint green circles. Arrows indicate proton fluxes, with their color indicating if ^{2}H fractionation potentially happens (orange) or not (black) during the process. During the light-dependent reactions (1–7), ^{2}H fractionation can potentially occur during: (1) the splitting of water molecules by the water-splitting complex (WSC) of photosystem II (PSII; Ferreira *et al*., 2004), which initially produces the protons for the whole reaction chain; (2) the exchange reaction between the free protons and the water molecules of the thylakoid lumen; (3) the proton pump of ATP synthase (ATPS; Seelert *et al*., 2000), which pumps protons from the thylakoid lumen into the chloroplast stroma as the δ^2H of the proton pool in the chloroplast stroma can potentially be influenced by a selective H^+ transport by ATPS; (4) the exchange reaction between the free protons and the water molecules of the chloroplast stroma; (5) the transfer of protons back into the thylakoid lumen by the cytochrome b 6 f complex (Cb 6fC; Cramer *et al*., 2011); (6) NADPH synthesis by ferredoxin-NADP $^+$ reductase (FNR; Nelson & Ben-Shem, 2005), which is connected to photosystem I (PSI) and uses protons from the pool in the chloroplast stroma. This process is driven by (7) the light-dependent reactions in the thylakoid. During the light-independent reactions (8–13), the δ^2H of the (8) proton pool in the chloroplast stroma is incorporated during the carbon dioxide (CO_2) assimilation process and probably further altered by ^{2}H fractionation. (9) About 75% of RuBisCO binds CO_2 to 3-phosphoglyceric acid (3-PGA). (10) About 25% of RuBisCO binds oxygen (O_2) in a process called photorespiration (Busch, 2020) and needs to be regenerated as 2-phosphoglycolate (2-PG) to form (11) 3-PGA (Bauwe, 2018). At least 82% of the 3-PGA pool comes from direct CO_2 fixation, while a maximum of 18% comes from photorespiration (Busch, 2020). Further biochemical exchange reactions involving H occur during (12) the Calvin–Benson–Bassham cycle (CBB), and (13) the synthesis of glucose-6-phosphate (G6P) out of glyceraldehyde-3-phosphate (G3P).

(up to 3% under normal conditions), RuBP (max. 29%), or from the water inside the chloroplasts' stroma (min. 50%; Cormier *et al*., 2018). NADPH is formed with protons from the pool in the chloroplast stroma, and thus might have a δ^2H similar to that in this water pool. This means, in summary, that up to 71% of the C-bound H in G6P is derived from the water inside the chloroplasts' stroma. Thus, the strong overall ^{2}H fractionation we observed is most likely driven by processes during the light-dependent reaction of photosynthesis. The most likely protein candidates causing the strong autotrophic ^{2}H fractionation, leading to ^{2}H-depleted sugars in C_3 plants, are therefore the water-splitting complex (WSC), ATP synthase (ATPS), the cytochrome b_6f complex (Cb_6fC), and ferredoxin-NADP$^+$ reductase (FNR).

The processes behind the heterotrophic ^{2}H fractionation, which caused the observed ^{2}H enrichment from leaf sugars to

twig xylem cellulose, most likely involve further steps that can be temporally and spatially separated from each other. For instance, trees form their tree rings at night, while sugars are formed during the day (Zweifel *et al.*, 2021). The very weak explanatory power of the δ^2H of twig xylem water for the δ^2H_{ne} of twig xylem cellulose ($R^2 = 0.1$) in our study indicates that the ^2H enrichment during cellulose formation was likely not caused by isotopic exchange with source water. Respiration has been identified as one heterotrophic ^2H-enriching process (Holloway-Phillips *et al.*, 2022). As plants respire continuously in all their living tissues, this accumulated respiratory ^2H enrichment in the leaves and twigs we sampled probably cause higher (less negative) δ^2H_{ne} in older pools of active carbohydrates, and with it higher δ^2H_{ne} of the cellulose that is formed from this pool (Lehmann *et al.*, 2021). In addition, trees and shrubs can be classified into the so-called 'starch' and 'fat' trees/shrubs (Kramer & Kozlowski, 1960), with the latter using more lipids, in addition to carbohydrates, for their energy storage (Hoch *et al.*, 2003; Herrera-Ramírez *et al.*, 2021). This variation in the use of storage compounds might explain some of the observed variation in the heterotrophic fractionation. However, as this classification according to storage compounds has not been done for a large fraction of species, further studies are needed to further explore the impact of such internal C dynamics.

^2H fractionation as a proxy for plants' metabolic properties

The strength of the ^2H fractionation differs between C_3, C_4, and CAM photosynthesis pathways (Sternberg *et al.*, 1984; Luo & Sternberg, 1991), with carbohydrates of C_3 plants being ^2H depleted compared with those of C_4 and CAM plants. Within our data set, the angiosperm species *Ilex aquifolium* stood out, with the highest ε_{HA}, and with two out of three sampled trees showing a ^2H enrichment instead of the typical ^2H depletion during sugar formation. Likewise, ε_{HE} of *Ilex aquifolium* was the only negative value among our tested species, leading to a more ^2H-depleted cellulose compared with the currently synthetized leaf sugar. A similar pattern has been observed previously in the CAM orchid *Phalaenopsis* BLUME, probably caused by C_3 photosynthesis during leaf formation and a subsequent switch to CAM photosynthesis when the leaves reached maturity (Schuler *et al.*, 2022). Thus, *Ilex aquifolium* might be an overlooked facultative CAM species. As increased respiration rates also correlate with ^2H enrichment (Holloway-Phillips *et al.*, 2022), strong respiration rates in *Ilex aquifolium* might drive the strong ^2H enrichment in its leaf sugars. In any case, the metabolism of this species appeared to be distinct from other tree species and deserves further study. In conclusion, screening δ^2H_{ne} of carbohydrates in different plant species has the potential to reveal unknown metabolic functional groups, such as C3–CAM intermediates, which cannot be identified by traditional isotope approaches (Edwards, 2019).

Conclusion

Our study highlights that (1) plant metabolism was the main driver of ^2H fractionation in plant carbohydrates, (2) plants' phylogeny strongly influenced the processes affecting δ^2H_{ne} at the leaf level, (3) ^2H fractionation processes influencing the δ^2H_{ne} of cellulose altered the initial phylogenetic signal found in δ^2H_{ne} within leaf sugars, (4) species-specific variability in ^2H fractionation must be taken into account if new ^2H fractionation models are to be developed, and (5) studying the ^2H fractionation between leaf water, leaf sugars and twig xylem cellulose could be used as a new tool for large-scale screening of plants' metabolic functioning. Based on our findings, we speculate that investigating the phylogenetic relationships of the proteins involved in the light-dependent reactions (WSC, ATPS, Cb_6fC, and FNR) might reveal the steps crucial for autotrophic ^2H fractionation. Finally, further studies are needed to investigate the interaction between ^2H fractionation factors and plant physiological processes, such as gas exchange rates, photorespiration, and plant internal carbon allocation in response to environmental forcing.

Acknowledgements

We thank Yvonne Aellen und Thierry Giegelmann from Basel city gardening (Stadtgärtnerei Basel) for granting us permission to sample the outstanding tree and shrub collection in Kannenfeldpark. We thank Manuela Oettli, Oliver Rehmann and Manuela Gjoka (all at WSL) for their laboratory assistance. We also thank Melissa Dawes (Dawes Scientific Editing) for proof-editing this manuscript. Our work was supported by the Swiss National Science Foundation (SNSF) Ambizione project TreeCarbo (no. 179978, granted to MML). Open access funding provided by ETH-Bereich Forschungsanstalten.

Competing interests

None declared.

Author contributions

PS and MML conceived and designed the study. PS, VV, MS and MML collected the samples. PS analyzed the data and led the writing of the manuscript. VV supported the analysis. PS, VV, MS, MML, AG and NB critically contributed to the manuscript and gave final approval for publication.

ORCID

Nina Buchmann https://orcid.org/0000-0003-0826-2980
Arthur Gessler https://orcid.org/0000-0002-1910-9589
Marco M. Lehmann https://orcid.org/0000-0003-2962-3351
Matthias Saurer https://orcid.org/0000-0002-3954-3534
Philipp Schuler https://orcid.org/0000-0002-5711-2535
Valentina Vitali https://orcid.org/0000-0003-0275-1310

Data availability

All data used in this manuscript are available in the Supporting Information.

References

Allen JF, De Paula WB, Puthiyaveetil S, Nield J. 2011. A structural phylogenetic map for chloroplast photosynthesis. *Trends in Plant Science* **16**: 645–655.

Arosio T, Ziehmer MM, Nicolussi K, Schlüchter C, Leuenberger M. 2020a. Alpine Holocene tree-ring dataset: age-related trends in the stable isotopes of cellulose show species-specific patterns. *Biogeosciences* **17**: 4871–4882.

Arosio T, Ziehmer-Wenz M, Nicolussi K, Schlüchter C, Leuenberger M. 2020b. Larch cellulose shows significantly depleted hydrogen isotope values with respect to evergreen conifers in contrast to oxygen and carbon isotopes. *Frontiers in Earth Science* **8**: 523073.

Augusti A, Betson TR, Schleucher J. 2006. Hydrogen exchange during cellulose synthesis distinguishes climatic and biochemical isotope fractionations in tree rings. *New Phytologist* **172**: 490–499.

Augusti A, Betson TR, Schleucher J. 2008. Deriving correlated climate and physiological signals from deuterium isotopomers in tree rings. *Chemical Geology* **252**: 1–8.

Baan J, Holloway-Phillips M, Nelson DB, Kahmen A. 2023. The metabolic sensitivity of hydrogen isotope fractionation differs between plant compounds. *Phytochemistry* **207**: 113563.

Badea S-L, Botoran OR, Ionete RE. 2021. Recent progresses in stable isotope analysis of cellulose extracted from tree rings. *Plants* **10**: 2743.

Barbeta A, Gimeno TE, Clavé L, Fréjaville B, Jones SP, Delvigne C, Wingate L, Ogée J. 2020. An explanation for the isotopic offset between soil and stem water in a temperate tree species. *New Phytologist* **227**: 766–779.

Bauwe H. 2018. Photorespiration—Damage repair pathway of the Calvin-Benson cycle. *Annual Plant Reviews* **50**: 293–342.

Brodribb TJ, Holbrook NM, Zwieniecki MA, Palma B. 2005. Leaf hydraulic capacity in ferns, conifers and angiosperms: impacts on photosynthetic maxima. *New Phytologist* **165**: 839–846.

Busch FA. 2020. Photorespiration in the context of Rubisco biochemistry, CO_2 diffusion and metabolism. *The Plant Journal* **101**: 919–939.

Cameron KM, Carmen Molina M. 2006. Photosystem II gene sequences of psbB and psbC clarify the phylogenetic position of *Vanilla* (Vanilloideae, Orchidaceae). *Cladistics* **22**: 239–248.

Cernusak LA, Barbeta A, Bush RT, Eichstaedt R, Ferrio JP, Flanagan LB, Gessler A, Martín-Gómez P, Hirl RT, Kahmen A. 2022. Do ^{2}H and ^{18}O in leaf water reflect environmental drivers differently? *New Phytologist* **235**: 41–51.

Cernusak LA, Barbour MM, Arndt SK, Cheesman AW, English NB, Feild TS, Helliker BR, Holloway-Phillips MM, Holtum JAM, Kahmen A *et al.* 2016. Stable isotopes in leaf water of terrestrial plants. *Plant, Cell & Environment* **39**: 1087–1102.

Cernusak LA, Farquhar GD, Pate JS. 2005. Environmental and physiological controls over oxygen and carbon isotope composition of Tasmanian blue gum, *Eucalyptus globulus*. *Tree Physiology* **25**: 129–146.

Coplen TB. 2011. Guidelines and recommended terms for expression of stable-isotope-ratio and gas-ratio measurement results. *Rapid Communications in Mass Spectrometry* **25**: 2538–2560.

Cormier M-A, Werner RA, Sauer PE, Gröcke DR, Leuenberger MC, Wieloch T, Schleucher J, Kahmen A. 2018. ^{2}H-fractionations during the biosynthesis of carbohydrates and lipids imprint a metabolic signal on the $\delta^{2}H$ values of plant organic compounds. *New Phytologist* **218**: 479–491.

Craig H. 1961. Isotopic variations in meteoric waters. *Science* **133**: 1702–1703.

Cramer WA, Hasan SS, Yamashita E. 2011. The Q cycle of cytochrome bc complexes: a structure perspective. *Biochimica et Biophysica Acta (BBA)–Bioenergetics* **1807**: 788–802.

Dansgaard W. 1964. Stable isotopes in precipitation. *Tellus* **16**: 436–468.

De Las Rivas J, Roman A. 2005. Structure and evolution of the extrinsic proteins that stabilize the oxygen-evolving engine. *Photochemical & Photobiological Sciences* **4**: 1003–1010.

Diao H, Schuler P, Goldsmith GR, Siegwolf RT, Saurer M, Lehmann MM. 2022. On uncertainties in plant water isotopic composition following extraction by cryogenic vacuum distillation. *Hydrology and Earth System Sciences* **26**: 5835–5847.

Dirghangi SS, Pagani M. 2013. Hydrogen isotope fractionation during lipid biosynthesis by *Haloarcula marismortui*. *Geochimica et Cosmochimica Acta* **119**: 381–390.

Edwards EJ. 2019. Evolutionary trajectories, accessibility and other metaphors: the case of C_4 and CAM photosynthesis. *New Phytologist* **223**: 1742–1755.

Epstein S, Thompson P, Yapp CJ. 1977. Oxygen and hydrogen isotopic ratios in plant cellulose. *Science* **198**: 1209–1215.

Falkner G, Horner F, Werdan K, Heldt HW. 1976. pH changes in the cytoplasm of the blue-green alga *Anacystis nidulans* caused by light-dependent proton flux into the thylakoid space. *Plant Physiology* **58**: 717–718.

Farquhar GD, Cernusak LA, Barnes B. 2007. Heavy water fractionation during transpiration. *Plant Physiology* **143**: 11–18.

Ferreira KN, Iverson TM, Maghlaoui K, Barber J, Iwata S. 2004. Architecture of the photosynthetic oxygen-evolving center. *Science* **303**: 1831–1838.

Filot MS, Leuenberger M, Pazdur A, Boettger T. 2006. Rapid online equilibration method to determine the D/H ratios of non-exchangeable hydrogen in cellulose. *Rapid Communications in Mass Spectrometry* **20**: 3337–3344.

Flexas J, Carriquí M. 2020. Photosynthesis and photosynthetic efficiencies along the terrestrial plant's phylogeny: lessons for improving crop photosynthesis. *The Plant Journal* **101**: 964–978.

Gehre M, Geilmann H, Richter J, Werner R, Brand W. 2004. Continuous flow $^{2}H/^{1}H$ and $^{18}O/^{16}O$ analysis of water samples with dual inlet precision. *Rapid Communications in Mass Spectrometry* **18**: 2650–2660.

Gessler A, Brandes E, Buchmann N, Helle G, Rennenberg H, Barnard RL. 2009. Tracing carbon and oxygen isotope signals from newly assimilated sugars in the leaves to the tree-ring archive. *Plant, Cell & Environment* **32**: 780–795.

Giguere PA. 1979. The great fallacy of the H^{+} ion: and the true nature of H_3O^{+}. *Journal of Chemical Education* **56**: 571.

Hadley JL. 2000. Effect of daily minimum temperature on photosynthesis in eastern hemlock (*Tsuga canadensis* L.) in autumn and winter. *Arctic, Antarctic, and Alpine Research* **32**: 368–374.

Heldt H. 1980. Measurement of metabolite movement across the envelope and of the pH in the stroma and the thylakoid space in intact chloroplasts. *Methods in Enzymology* **69**: 604–613.

Heldt HW, Werdan K, Milovancev M, Geller G. 1973. Alkalization of the chloroplast stroma caused by light-dependent proton flux into the thylakoid space. *Biochimica et Biophysica Acta (BBA)–Bioenergetics* **314**: 224–241.

Herrera-Ramírez D, Muhr J, Hartmann H, Römermann C, Trumbore S, Sierra CA. 2020. Probability distributions of nonstructural carbon ages and transit times provide insights into carbon allocation dynamics of mature trees. *New Phytologist* **226**: 1299–1311.

Herrera-Ramírez D, Sierra CA, Römermann C, Muhr J, Trumbore S, Silvério D, Brando PM, Hartmann H. 2021. Starch and lipid storage strategies in tropical trees relate to growth and mortality. *New Phytologist* **230**: 139–154.

Hoch G, Richter A, Körner C. 2003. Non-structural carbon compounds in temperate forest trees. *Plant, Cell & Environment* **26**: 1067–1081.

Holloway-Phillips M, Baan J, Nelson DB, Lehmann MM, Tcherkez G, Kahmen A. 2022. Species variation in the hydrogen isotope composition of leaf cellulose is mostly driven by isotopic variation in leaf sucrose. *Plant, Cell & Environment* **45**: 2636–2651.

Kagawa A. 2022. Foliar water uptake as a source of hydrogen and oxygen in plant biomass. *Tree Physiology* **42**: 2153–2173.

Kagawa A, Battipaglia G. 2022. Post-photosynthetic carbon, oxygen and hydrogen isotope signal transfer to tree rings—how timing of cell formations and turnover of stored carbohydrates affect intra-annual isotope variations. In: *Stable isotopes in tree rings: inferring physiological, climatic and environmental responses*. Tree Physiology *vol.* **8**. Cham, Switzerland: Springer Nature, 429–462.

Karlusich JJP, Carrillo N. 2017. Evolution of the acceptor side of photosystem I: ferredoxin, flavodoxin, and ferredoxin-$NADP^{+}$ oxidoreductase. *Photosynthesis Research* **134**: 235–250.

Kramer PJ, Kozlowski TT. 1960. *Physiology of trees*. New York, NY, USA: McGraw-Hill.

Lehmann MM, Egli M, Brinkmann N, Werner RA, Saurer M, Kahmen A. 2020. Improving the extraction and purification of leaf and phloem sugars for oxygen isotope analyses. *Rapid Communications in Mass Spectrometry* **34**: e8854.

Lehmann MM, Goldsmith GR, Schmid L, Gessler A, Saurer M, Siegwolf RT. 2018. The effect of ^{18}O-labelled water vapour on the oxygen isotope ratio of water and assimilates in plants at high humidity. *New Phytologist* **217**: 105–116.

Lehmann MM, Schuler P, Cormier M-A, Allen ST, Leuenberger M, Voelker S. 2022. The stable hydrogen isotopic signature: from source water to tree rings. In: *Stable isotopes in tree rings: inferring physiological, climatic and environmental responses*. Tree Physiology *vol.* **8**. Cham, Switzerland: Springer Nature, 331–359.

Lehmann MM, Vitali V, Schuler P, Leuenberger M, Saurer M. 2021. More than climate: hydrogen isotope ratios in tree rings as novel plant physiological indicator for stress conditions. *Dendrochronologia* **65**: 125788.

Luo Y-H, Steinberg L, Suda S, Kumazawa S, Mitsui A. 1991. Extremely low D/H ratios of photoproduced hydrogen by cyanobacteria. *Plant and Cell Physiology* **32**: 897–900.

Luo Y-H, Sternberg L. 1991. Deuterium heterogeneity in starch and cellulose nitrate of CAM and C_3 plants. *Phytochemistry* **30**: 1095–1098.

Lusk CH, Wright I, Reich PB. 2003. Photosynthetic differences contribute to competitive advantage of evergreen angiosperm trees over evergreen conifers in productive habitats. *New Phytologist* **160**: 329–336.

Molina-Venegas R, Rodríguez MÁ. 2017. Revisiting phylogenetic signal; strong or negligible impacts of polytomies and branch length information? *BMC Evolutionary Biology* **17**: 1–10.

Nabeshima E, Nakatsuka T, Kagawa A, Hiura T, Funada R. 2018. Seasonal changes of δD and $\delta^{18}O$ in tree-ring cellulose of *Quercus crispula* suggest a change in post-photosynthetic processes during earlywood growth. *Tree Physiology* **38**: 1829–1840.

Nelson N, Ben-Shem A. 2005. The structure of photosystem I and evolution of photosynthesis. *BioEssays* **27**: 914–922.

Palacio S, Camarero JJ, Maestro M, Alla AQ, Lahoz E, Montserrat-Martí G. 2018. Are storage and tree growth related? Seasonal nutrient and carbohydrate dynamics in evergreen and deciduous Mediterranean oaks. *Trees* **32**: 777–790.

Patterson AE, Arkebauer R, Quallo C, Heskel MA, Li X, Boelman N, Griffin KL. 2018. Temperature response of respiration and respiratory quotients of 16 co-occurring temperate tree species. *Tree Physiology* **38**: 1319–1332.

Pedersen TL. 2022. PATCHWORK: the composer of plots. [WWW document] URL https://github.com/thomasp85/patchwork [accessed 17 May 2023].

R Core Team. 2021. *R: A language and environment for statistical computing*. Vienna, Austria: R Foundation for Statistical Computing.

Recipon H, Perasso R, Adoutte A, Quetier F. 1992. ATP synthase subunit c/III/9 gene sequences as a tool for interkingdom and metaphytes molecular phylogenies. *Journal of Molecular Evolution* **34**: 292–303.

Revell LJ. 2012. PHYTOOLS: an R package for phylogenetic comparative biology (and other things). *Methods in Ecology and Evolution* **3**: 217–223.

Rinne KT, Saurer M, Streit K, Siegwolf RT. 2012. Evaluation of a liquid chromatography method for compound-specific $\delta^{13}C$ analysis of plant carbohydrates in alkaline media. *Rapid Communications in Mass Spectrometry* **26**: 2173–2185.

Roden JS, Ehleringer JR. 1999. Hydrogen and oxygen isotope ratios of tree-ring cellulose for riparian trees grown long-term under hydroponically controlled environments. *Oecologia* **121**: 467–477.

Roden JS, Ehleringer JR. 2000. Hydrogen and oxygen isotope ratios of tree ring cellulose for field-grown riparian trees. *Oecologia* **123**: 481–489.

Roden JS, Lin G, Ehleringer JR. 2000. A mechanistic model for interpretation of hydrogen and oxygen isotope ratios in tree-ring cellulose. *Geochimica et Cosmochimica Acta* **64**: 21–35.

Sanchez-Bragado R, Serret MD, Marimon RM, Bort J, Araus JL. 2019. The hydrogen isotope composition δ^2H reflects plant performance. *Plant Physiology* **180**: 793–812.

Schaberg P. 2000. Winter photosynthesis in red spruce (*Picea rubens* Sarg.): limitations, potential benefits, and risks. *Arctic, Antarctic, and Alpine Research* **32**: 375–380.

Scheiner S, Čuma M. 1996. Relative stability of hydrogen and deuterium bonds. *Journal of the American Chemical Society* **118**: 1511–1521.

Schönbeck LC, Santiago LS. 2022. Time will tell: towards high resolution temporal tree-ring isotope analyses. *Tree Physiology* **42**: 2401–2403.

Schuler P, Cormier MA, Werner RA, Buchmann N, Gessler A, Vitali V, Saurer M, Lehmann MM. 2022. A high temperature water vapor equilibration method to determine non-exchangeable hydrogen isotope ratios of sugar, starch, and cellulose. *Plant, Cell & Environment* **45**: 12–22.

Seelert H, Poetsch A, Dencher NA, Engel A, Stahlberg H, Müller DJ. 2000. Proton-powered turbine of a plant motor. *Nature* **405**: 418–419.

Shirao M, Kuroki S, Kaneko K, Kinjo Y, Tsuyama M, Förster B, Takahashi S, Badger MR. 2013. Gymnosperms have increased capacity for electron leakage to oxygen (Mehler and PTOX reactions) in photosynthesis compared with angiosperms. *Plant and Cell Physiology* **54**: 1152–1163.

Sternberg L, Deniro MJ, Ajie H. 1984. Stable hydrogen isotope ratios of saponifiable lipids and cellulose nitrate from Cam, C_3 and C_4 plants. *Phytochemistry* **23**: 2475–2477.

Tixier A, Orozco J, Roxas AA, Earles JM, Zwieniecki MA. 2018. Diurnal variation in nonstructural carbohydrate storage in trees: remobilization and vertical mixing. *Plant Physiology* **178**: 1602–1613.

Vitali V, Martínez-Sancho E, Treydte K, Andreu-Hayles L, Dorado-Liñán I, Gutierrez E, Helle G, Leuenberger M, Loader NJ, Rinne-Garmston KT. 2022. The unknown third–Hydrogen isotopes in tree-ring cellulose across Europe. *Science of the Total Environment* **813**: 152281.

West AG, Patrickson SJ, Ehleringer JR. 2006. Water extraction times for plant and soil materials used in stable isotope analysis. *Rapid Communications in Mass Spectrometry* **20**: 1317–1321.

West JB, Sobek A, Ehleringer JR. 2008. A simplified GIS approach to modeling global leaf water isoscapes. *PLoS ONE* **3**: e2447.

White J. 1989. Stable hydrogen isotope ratios in plants: a review of current theory and some potential applications. In: *Ecological studies, vol.* **68**. New York, NY, USA: Springer-Verlag, 142–162.

Wickham H. 2016. *GGPLOT2: elegant graphics for data analysis*. New York, NY, USA: Springer-Verlag. [WWW document] URL https://ggplot2.tidyverse.org [accessed 21 November 2022].

Wieloch T, Grabner M, Augusti A, Serk H, Ehlers I, Yu J, Schleucher J. 2022. Metabolism is a major driver of hydrogen isotope fractionation recorded in tree-ring glucose of *Pinus nigra*. *New Phytologist* **234**: 449–461.

Yapp CJ, Epstein S. 1982. Climatic significance of the hydrogen isotope ratios in tree cellulose. *Nature* **297**: 636–639.

Zhang Y, Cao K, Goldstein G. 2013. Winter photosynthesis of evergreen broadleaf trees from a montane cloud forest in subtropical China. In: *Photosynthesis research for food, fuel and the future*. Heidelberg, Germany: Springer, 812–817.

Zhou Y, Grice K, Stuart-Williams H, Hocart CH, Gessler A, Farquhar GD. 2016. Hydrogen isotopic differences between C_3 and C_4 land plant lipids: consequences of compartmentation in C_4 photosynthetic chemistry and C_3 photorespiration. *Plant, Cell & Environment* **39**: 2676–2690.

Ziegler H. 1989. Hydrogen isotope fractionation in plant tissues. In: *Stable isotopes in ecological research, vol. 68*. New York, NY, USA: Springer-Verlag, 105–123.

Zweifel R, Sterck F, Braun S, Buchmann N, Eugster W, Gessler A, Häni M, Peters RL, Walthert L, Wilhelm M. 2021. Why trees grow at night. *New Phytologist* **231**: 2174–2185.

Supporting Information

Additional Supporting Information may be found online in the Supporting Information section at the end of the article.

Fig. S1 Pagel's λ of δ^2H_{ne} leaf sugars and ε_{HA}.

Fig. S2 Pagel's λ of δ^2H_{ne} twig xylem cellulose and ε_{HE}.

Fig. S3 Pagel's λ of δ^2H twig xylem water, δ^2H leaf water, and leaf water enrichment.

Fig. S4 Violin plots of δ^2H_{ne} of leaf sugars, ε_{HA}, δ^2H_{ne} of twig xylem cellulose, ε_{HE}, δ^2H of twig xylem water, δ^2H of leaf water,

and leaf water enrichment between deciduous and evergreen angiosperms and gymnosperms.

Table S1 List of all sampled trees and shrubs and their scientific classification.

Table S2 Temperature (°C) and humidity (RH%) during the 2 d of measurements.

Table S3 δ^2H measurements and calculation of the δ^2H_{ne} of the extracted leaf sugar.

Table S4 δ^2H measurements and calculation of the δ^2H_{ne} of the extracted twig xylem cellulose.

Table S5 Average δ^2H and δ^2H_{ne} values per species including standard deviation (SD), the ^2H fractionation factors εHA and εHE, and the leaf water enrichment (LWE).

Table S6 Results of the analysis of variance comparing the δ^2H and δ^2H_{ne} values, the ^2H fractionation factors ε_{HA} and ε_{HE}, and the leaf water enrichment (LWE) of the different phylogenetic groups, from the order to the family level.

Please note: Wiley is not responsible for the content or functionality of any Supporting Information supplied by the authors. Any queries (other than missing material) should be directed to the *New Phytologist* Central Office.